Control of Complexity Constraints on Combinatorial Screening for Preferred Oligonucleotide Hybridization Sites on Structured RNA

Thomas W. Bruice*,‡,§ and Walt F. Lima§

Departments of Research Medicinal Chemistry and Molecular, Cellular and Structural Biology, Isis Pharmaceuticals, 2292 Faraday Avenue, Carlsbad, California 92008

Received August 16, 1996; Revised Manuscript Received December 23, 1996⊗

ABSTRACT: We have explored the use of short (10-mer), fully sequence-randomized oligonucleotide libraries for affinity-based screening in solution for energetically preferred sites of hybridization of a model 47-nucleotide (nt) mutant Ha-*ras* mRNA stem−loop fragment. In characterizing the model, binding studies using either a gel mobility-shift assay or an RNase ONE footprinting assay indicated the presence of a greatly preferred hybridization site for individual antisense RNA oligonucleotides on the 5′-most side of the *ras* RNA 19-nt loop. However, initial attempts to affinity-titrate combinatorial uniform 2′-O-methyl-substituted oligonucleotide libraries for selective binding to this 5′-loop site using an RNase ONE footprinting assay that can discriminate between binding to different sites on *ras* RNA were unsuccessful. By reducing the complexity of the library to a mix of seven RNA oligonucleotides complementary to a range of sites on *ras* RNA and with no self-complements, footprinting evidence for binding was obtained but was characterized by *ras* RNA site-specific binding constants differing dramatically from binding constants for individual oligonucleotides. The library complexity was reduced further to three different cases of two RNA oligonucleotides, one of which for all cases was the highest affinity 5′-loop complement. Detailed kinetic and thermodynamic binding analyses revealed a good fit of the data to independent (5′-loop and ascending stem sites), competitive (overlapping 5′-loop sites), or mutually allosteric (5′-loop and 3′-loop sites) formalisms and an energetics description showed that *ras* 5′-loop site-specific binding could be achieved by affinity titration only for the independent case. Reconstruction of events with the full complexity library suggested that there was the emergence of multiple, linked binding interactions and implied that successful hybridization affinity screening would be achieved only if all possible bimolecular binding interactions of individual library oligonucleotides with target RNA could be made mutually independent. Accordingly, by holding the calculated concentration of unique oligonucleotide sequences of a full complexity DNA library well below the value for the dissociation constant for binding of individual complement to the 5′-loop site and then titrating the concentration of *ras* RNA through this value, hybridization specific to the 5′-side of the *ras* loop was demonstrated as assayed either by sequential gel mobility-shift resolution of bimolecular complexes and RNase ONE footprinting *in situ* in gel slices or by RNase H cleavage of complexes in solution. Because this strategy uses an unbiased oligonucleotide library it should combinatorially identify energetically preferred hybridization sites on folded RNA targets of any sequence and of undetermined structure. This should enable a focused *in vitro* optimization of antisense oligonucleotide length, sequence, and chemical composition for preferred site binding affinity and specificity which, in turn, may be expected to provide for enhanced biological potency and specificity (Lima et al., 1996). Finally, the complexity constraints encountered and the fundamental requirement to control them presented here also should be applicable to interactions with any biomolecule target of any chemical class of combinatorial library when screened in solution in pooled mixes.

Both the kinetics and the thermodynamics of antisense and ribozyme oligonucleotide hybridization may be profoundly attenuated when an energetic cost is incurred to disrupt secondary and tertiary structures of folded transcript RNA that block the hybridization (Lima et al., 1992; Chastain & Tinoco, 1993; Freier, 1993; Nellen & Lichtenstein, 1993). The complexity of folded RNA suggests that there should be great variability of RNA structure-dependent hybridization parameters for oligonuclotides complementary to different positions along the primary sequence. In addition, examination of known RNA secondary structure reveals the improbability of identifying structurally ideal RNA hybridization sites for oligonucleotides as long as 20-mers,[1] which has been a theoretically (Cohen & Hogan, 1994; Wu-Pong, 1994) and operationally (Chiang et al., 1991; Dean et al., 1994) favored length. Therefore, it should be expected that typical piecemeal sampling ("walks") at chosen intervals along linear RNA transcript sequences with a manageable set (*ca.* 10−50) of complementary 20-mer oligonucleotides (Chiang et al., 1991; Dean et al., 1994) generally will identify perhaps

* Corresponding author. Current address: Department of Biochemistry and Biophysics, Genelabs Technologies, 505 Penobscot Dr., Redwood City, CA 94063. Tel, (415) 562-1448; Fax, (415) 368-3198; E-mail, tbruice@genelabs.com.

‡ Department of Research Medicinal Chemistry.

§ Department of Molecular, Cellular and Structural Biology.

⊗ Abstract published in *Advance ACS Abstracts,* April 1, 1997.

[1] Abbreviations: nt, nucleotide; -mer, oligomer; oligo, oligonucleotide; PAGE, polyacrylamide gel electrophoresis; PCR, polymerase chain reaction; 2′-OMe, 2′-deoxy, 2′-O-methyl; CPG, controlled pore glass; DMT, dimethoxytrityl; DTT, dithiothreitol; RP-HPLC, reverse-phase high-performance liquid chromatography.

S0006-2960(96)02076-4 CCC: $14.00

a few that give sufficient net binding affinity, after disruption of RNA structure, to support adequate activity in biological screens. Oligonucleotides chosen in this manner may further be expected to bind with near to, equivalent, or even higher affinity at alternative RNA sites on the same or other transcript(s) that are closely sequence-related but more favorably structured. At effective antisense oligonucleotide concentrations, this will result in diminished hybridization site and transcript specificity (Woolf et al., 1992; Stein & Krieg, 1994; Wagner, 1994; Weidner & Busch, 1994; Jones et al., 1996).

Efforts to advance design of antisense oligonucleotides beyond the "linear thinking" of sequence complementarity have included computer RNA folding algorithms as well as enzymatic and chemical reagent mapping approaches used to determine RNA secondary structure. These procedures are tedious to perform, do not predict tertiary interactions, and may be unreliable (Jaeger et al., 1993; Jaroszewski et al., 1993; Sczakiel et al., 1993). When single-stranded regions of RNA are accurately located, there may be errors of many orders of magnitude in subsequent indirect predictions for the kinetics and thermodynamics of complementary oligonucleotide hybridization due to steric, topological, and tertiary structural constraints not evident in secondary structure determinations (Lima et al., 1992). There has been some early-stage success in enhancing hybridization of antisense oligonucleotides to transcripts by rational design, including the use of tethered oligonucleotide probes (Cload & Schepartz, 1991; Richardson & Schepartz, 1991; Cload et al., 1993), pseudo-half-knots (Ecker et al., 1992; Ecker, 1993), symmetric secondary structures (Chang & Tinoco, 1994; Frauendorf & Engels, 1994), and stem-bridging (Francois et al., 1994). However, these approaches all require identification of particular RNA structural elements and are limited in scope when viewed against the potential structural diversity of available RNA targets in cells. Most recently, potentially powerful combinatorial or semicombinatorial strategies that do not depend on predetermined knowledge of RNA structure have been applied to the problem of oligonucleotide recognition of folded RNA. Although (partial) randomization of the RNA substrate recognition nucleotides of *trans*-cleaving ribozymes (Campbell & Cech, 1995; Lieber & Strauss, 1995) is promising, the methodology is not directly applicable to smaller antisense oligonucleotides. Probing hybridization to structured RNA with multiple-length fragments of a given antisense nucleic acid generated by semicombinatorial solid-phase synthesis (Southern et al., 1994) or by solution-based alkaline fragmentation of end-labeled RNA (Rittner et al., 1993) represent innovative screening approaches. However, solid-phase screening may bias the former, conserved end fragments of the latter do not mimic therapeutic antisense oligonucleotides, and both methods require unique synthesis of (the equivalent of) full-length antisense nucleic acid for a complete search of a given RNA metabolite. All methods currently are subject to restrictions on the length of target RNA that can be accommodated, which may or may not be easily surmounted to eventually provide more efficient searches of long transcript RNAs.

There remains a need for general methods to directly identify oligonucleotides that hybridize to folded RNA of undetermined structure with minimal energetic cost (Ladbury & Peters, 1994) of disrupting RNA structure. Such oligonucleotides would maximize rates of hybridization (or "kinetic accessibility") and hence, as previously shown, also would maximize affinity per unit length (Lima et al., 1992) and effectiveness of *in vivo* antisense inhibition (Rittner et al., 1993) at the intended site of hybridization. Optimized RNA structure recognition should also provide enhanced specificity by reducing the probability of finding other close sequence-related RNA sites with structures as comparably favorable for oligonucleotide hybridization. Oligonucleotides with these properties most likely would be restricted by RNA structure to no more than 10−15 nt in length. These should demonstrate biological potency at least equivalent to that of 20-mer oligonucleotides of similar chemical design, because of the fullest possible realization of hybridization affinity (Wagner et al., 1996). The potential problem of formation of internal oligonucleotide structure, which would lessen the net hybridization affinity with RNA (Chastain & Tinoco, 1993), would also be minimized with shorter oligonucleotides. There are other potential advantages of shorter oligonucleotides, including enhancement of primary sequence mismatch specificity (Herschlag, 1991; Monia et al., 1992; Hertel et al., 1994) and product release after RNase-, ribozyme-, or artificial agent-mediated RNA cleavage (Hertel et al., 1994), improved cellular uptake (Loke et al., 1989), reduced nonspecific protein binding (Stein & Krieg, 1994), and less expensive synthesis and purification.

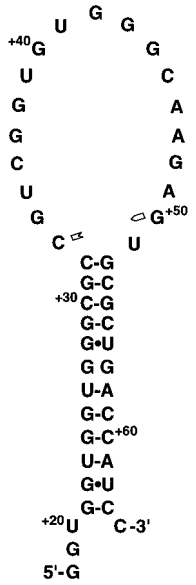

FIGURE 1: Consensus secondary structure of the 47-nt fragment corresponding to residues 18−64 of mutant Ha-*ras* mRNA. The depiction was constructed from combined data of previous mapping with multiple enzymes (not including RNase ONE) (Lima et al., 1992) and with RNase ONE in the absence of any added oligonucleotides (this study). Solid dashes between the one-letter designations of nucleotides indicate canonical Watson−Crick base pairing, solid dots indicate alternative base pairs, and no symbol indicates mismatched bases. The open and broken dash between C(33) and G(50) is meant to indicate evidence for the presence of partial double-strand and single-strand secondary structure at these nucleotides. The numbering system is as for the full-length mutant mRNA.

Here we report initial studies that explore the use of short (10-mer), fully sequence-randomized oligonucleotide libraries to combinatorially search all of sequence and structure space of any given RNA in order to identify energetically preferred sites of hybridization. A 47-nt mutant Ha-*ras* mRNA fragment (Figure 1) was used as a model target since it is a

previously studied (Lima et al., 1992) example of a ubiquitous RNA secondary structural element, the stem−loop, that is attractive for oligonucleotide hybridization (*i.e.*, at the loop) (Ecker et al., 1992).

MATERIALS AND METHODS

Preparation of ras Transcript Fragment. The DNA template for T7 RNA polymerase transcription was prepared using a standard method for PCR copying of a segment of the activated Ha-*ras* sequence of the plasmid pT24-C3 as described previously (Lima et al., 1992). The sense oligonucleotide PCR primer contained the 17-mer T7 RNA polymerase promoter followed by a 15-mer sequence homologous to nt +18 to +32 of Ha-*ras* mRNA and the antisense oligonucleotide primer was complementary to Ha-*ras* nt +50 to +64. The 47-nt transcript fragment from sequence position +18 to +64 of Ha-*ras* mRNA was prepared from the PCR-synthesized duplex DNA template using the Ambion MegaScript kit according to instructions (Lima et al., 1992) and was extracted with phenol−$CHCl_3$ and precipitated with ethanol and then purified using Boehringer-Mannheim G-50 quick spin columns as instructed.

Synthesis of Oligonucleotides and Randomized Oligonucleotide Libraries. DNA antisense oligonucleotides and PCR oligonucleotide primers were synthesized by standard phosphoramidite chemistry on an ABI synthesizer (Model 380B) and were purified by precipitation 2 times out of 0.5 M NaCl with 2.5 volumes of ethanol (Lima et al., 1992).

Antisense 2′-OMe oligonucleotides were synthesized by automated synthesis and were purified as described previously (Guinosso et al., 1991; Lesnik et al., 1993) using commercially available (Glenn Research) 2′-OMe phosphoramidites and a modified DNA synthesis cycle.

Oligoribonucleotides were synthesized using an ABI synthesizer (380B). Briefly, 5′-DMT 2′-(*t*-butyldimethylsilyl)nucleoside 3′-*O*-phosphoramidites with phenoxyacetyl protecting groups on the exocyclic amines of A, C, and G were used. The wait step after pulse delivery of tetrazole was 900 s. Base deprotection was achieved by overnight incubation at room temperature in methanolic ammonia and the 2′-silyl group was removed at room temperature in 1 M tetrabutylammonium fluoride in tetrahydrofuran. RNA oligonucleotides were purified using a C18 Sep-Pak cartridge followed by ethanol precipitation (Lima et al., 1992).

Fully randomized sequence DNA and 2′-OMe 10-mer combinatorial libraries were made using the same respective automated chemistries as described for individual oligonucleotides, but with the following modifications (Davis & Ecker, 1996) to ensure equimolar representation of all possible sequence oligonucleotides (calculated as $4^{10} = 1\,048\,576$ sequences). Equimolar incorporation of all four bases at each sequence position of the synthesis was obtained by mixing the phosphoramidites in a single vial on the fifth port of the ABI 394 synthesizer and increasing the coupling wait step to 5 min. The ratio of phosphoramidites in the mixture was tested by making a single coupling to dT-CPG, cleaving and deprotecting the product, and analyzing the crude dinucleotide material on RP-HPLC. Proportions of the individual phosphoramidites were adjusted accordingly and the procedure was repeated until equal amounts of the four dimers were obtained. The 3′-position was sequence-randomized by mixing the four base CPGs, removing the 5′-DMT on the synthesizer, cleaving and deprotecting the product, and analyzing by RP-HPLC. The proportion of each CPG was adjusted until equal amounts of each base were obtained. Each oligonucleotide library synthesis used 1 μM mixed-base CPG. After cleavage and deprotection with ammonium hydroxide at 55 °C for 16 h, the DMT-off oligonucleotide libraries were purified by RP-HPLC. The libraries were analyzed by denaturing PAGE and were diluted to a final library concentration of 10 μM. Limit hydrolyses by snake venom phosphodiesterase I (U.S. Biochemical Corp.) and examination of products by UV absorption on RP-HPLC confirmed the equimolar representation of bases. A few sequences may be underrepresented, without affecting this result, due to relatively poor aqueous solubility; *i.e.*, of long strings of G nucleotides.

^{32}P Labeling of RNA Transcript and Oligonucleotides. The RNA transcripts were dephosphorylated with calf intestinal alkaline phosphatase (Boehringer-Mannheim). The transcripts and oligonucleotides were 5′-end-labeled with ^{32}P using [γ-^{32}P]ATP (ICN Biochemicals) and T4 polynucleotide kinase (Promega) according to standard procedures (Lima et al., 1992). Labeled transcripts were purified by 8−12% denaturing PAGE and were extracted with phenol−$CHCl_3$ and precipitated with ethanol. Labeled oligonucleotides were purified using a C18 Sep-Pak. Specific activities were typically 2000−6000 cpm/fmol.

Determination of Binding Constants by Gel Mobility-Shift Assay. Equilibrium constants for hybridization of individual antisense oligonucleotides to the *ras* RNA hairpin were measured using a gel mobility-shift assay (Lima et al., 1992, 1997). Hybridizations were done in 20 μL containing hybridization buffer (1 mM Tris-HCl, pH 7.4, 50 mM NaCl, and 5 mM $MgCl_2$; use of 10 mM sodium phosphate, and 100 mM NaCl, pH 7.0, gave similar results) and 1000 cpm of 5′-^{32}P-labeled RNA (∼8 pM; 1−10 pM range). Mixes were heated at 90 °C for 5 min and cooled slowly to 37 °C, antisense oligonucleotide ranging from 1 pM to 10 μM was added, and final mixes were incubated for 20 h at 37 °C; some incubations proceeded for as long as 40 h with identical results. Loading buffer (15% Ficoll, 0.25% bromphenol blue, and 0.25% xylene cyanol) was added (10 μL) and mixes were resolved at 10 °C on native 20% PAGE using 44 mM Tris−borate and 1 mM $MgCl_2$ running buffer, for ∼4 h at 122 W. Gels were quantitatively imaged using a Molecular Dynamics Phosphorimager. The dissociation constant (K_d) was determined simply as the antisense oligonucleotide concentration at which 50% of the target is mobility-shifted, which is most accurate for K_d values greater than the concentration of RNA target. Limitations on the specific radioactivity of the target restricted values of K_a to an upper limit of $\sim 5 \times 10^{11}$ M^{-1}. The log linear range of the assay was determined (not shown) to cover from 50 pM to 10 mM in K_d values for antisense oligonucleotides. All binding constants were derived from the average of at least three independent determinations differing by at most 2−3-fold.

Determination of Binding Constants by RNase ONE Footprinting Assay. Equilibrium constants for hybridization also were determined using a footprinting assay with RNase ONE (Promega), a sequence-independent and single-strand-dependent endoribonuclease. Hybridization reactions were performed similarly as above in 10 μL containing hybridization buffer and 5000 cpm of 5′-^{32}P-labeled transcript (∼1−5

pM), which was heated and slow-cooled as above. Individual antisense oligonucleotides ranging from 1 pM to 10 μM were then added to the solutions. Hybridization reactions containing oligonucleotide mixtures were prepared by adding equimolar amounts of each sequence and titrating the individual sequence concentration in the mixes from 1 pM to 10 μM, with the exception of experiments in which one oligonucleotide sequence was titrated over an indicated range while another sequence was held at an indicated constant concentration. Hybridization reactions were incubated at 37 °C for 20 h (some for as long as 40 h). Hybridization reactions were digested with RNase ONE by adding 3 μg of tRNA and enzyme at a concentration (0.1−1.0 unit) empirically determined to result in less than 10% digestion over 5 min at 37 °C. Digestions were stopped by snap freezing on dry ice followed by addition of 5 μL of gel loading buffer [9 M urea (6 M final), 0.25% bromphenol blue, and 0.25% xylene cyanol) and products were resolved on denaturing 12% PAGE and were quantified by phosphorimaging. Binding curves were generated by plotting the percent protection from cleavage of the mean band intensity of all cleavable sequence positions within the footprintable hybridization site. The dissociation constants were determined from at least three experiments as the average oligonucleotide concentration giving 50% protection on binding curves; variance of values between experiments was within 2−3-fold.

Determination of Hybridization Rates. Hybridization association and dissociation rate constants were determined using the gel mobility-shift assay (Lima et al., 1992). For bimolecular association rates (k_n), hybridization reactions were prepared as described above except that a single antisense oligonucleotide concentration 10-fold over the K_d was used. Reactions were then incubated at 37 °C and quick-quenched by snap-freezing on dry ice at chosen time intervals and then run on native PAGE as above.

For dissociation rates (k_{-n}) the same concentration of antisense oligonucleotides as for association rate determinations was incubated with the 5′-end-labeled target RNA for 20 h at 37 °C. Following this equilibrium annealing, unlabeled target RNA was added in 10-fold excess over the antisense oligonucleotide and exchange reactions were allowed to proceed for prescribed intervals after which they were quenched and analyzed as described above.

RNase ONE Footprinting Assay for Combinatorial Hybridization Affinity Screening: Library Sequences in Excess of Transcript. Labeled transcript was prepared in hybridization buffer and heat-denatured and cooled as above for RNase ONE footprinting of single, or mixes of small numbers of, oligonucleotides. Randomized sequence oligonucleotide libraries were diluted in water, heat-denatured and cooled, and added to the hybridization reaction to a final library concentration of 500 μM to 5 mM. The hybridization incubations, RNase ONE digestions, and PAGE analyses were as described above for assays of single oligonucleotides.

RNase ONE Footprinting Assay, Post Gel Mobility-Shift Resolution, for Combinatorial Hybridization Affinity Screening: Transcript in Excess of Library Sequences. Hybridization reactions were prepared as described above with the exception that 100 μM oligonucleotide library and unlabeled transcript ranging in concentration from 100 pM to 500 nM were added; labeled transcript was added at the same concentration as above for all assays. The library and transcript were individually heat-denatured and slow-cooled and the hybridization reactions were incubated as described previously. The large excess of unhybridized transcript was resolved from hybridized transcript by gel mobility shift (Lima et al., 1992). The gel was exposed briefly (∼1 min) to autoradiography film (Kodak X-OMAT AR) to locate the band corresponding to unhybridized (free) transcript, which was excised and discarded. The gel was reexposed for a longer period (∼30 min) to locate the marginally resolved (Lima et al., 1992) band containing the hybridized (bound) transcript, which was excised and crushed. Then, 20 μL of hybridization buffer containing 5 units of RNase ONE was added to the crushed gel and the immersed gel pieces were incubated for 10 min at 24 °C. The digestion reactions were quenched by snap-freezing. Urea was added to 8 M and the supernatant was removed from the gel pieces on sterile spin-filter columns and digestion products were resolved on denaturing 12% PAGE as described previously.

RNase H Cleavage Assay for Combinatorial Hybridization Affinity Screening: Transcript in Excess of Library Sequences. Hybridization reactions were prepared and incubated as described above with the transcript concentration in excess of the concentration of individual oligonucleotide sequences in the DNA library. Hybridization reactions were digested by adding 1.0 unit of RNase H and 1 mM DTT and incubating for 10 min at 37 °C. The digestion reactions were quenched and products were resolved by denaturing PAGE as described above.

RESULTS

Binding of Individual Oligonucleotides to ras Transcript RNA. The gel mobility-shift assay was used to determine the individual oligonucleotide equilibrium binding constants of six different decaribonucleotides with the *ras* stem−loop RNA. The results are summarized in Figure 2A. The affinities of all decaribonucleotides are markedly dependent on the *ras* target site, which must reflect the effects of different target site structure much more than differences in sequence (Lima et al., 1992). Oligonucleotides targeting anywhere on the stem or on the extreme 3′-side of the loop exhibited 10^5−10^6-fold lower affinity than oligonucleotide 3291 targeting the far 5′-side of the loop. Oligonucleotide 3283 targeting the middle of the loop binds only 10-fold less well than 3291. The observed binding constant for 3291 may be stoichiometrically limited and the true value may therefore be of higher affinity.

Binding of individual decaribonucleotides to the *ras* stem−loop also was investigated using a transcript target site-specific RNase ONE footprinting assay. Figure 2B shows the results of binding titrations assayed by RNase ONE footprinting of the decaribonucleotides 3291 and 3284, which target the far left (5′-) and right (3′-) sides of the *ras* loop, respectively. For both oligonucleotides, footprints are clearly discernible. The footprint for the 3284 site is about the same size as the oligonucleotide (±1 nt) and is 2−3 nt longer than the oligonucleotide at the 3291 site. There are no products of cleavage of either the ascending or descending strands of the stem for titrations of either oligonucleotide up to the highest concentrations employed, indicating that full complementary sequence binding for either is not accompanied by any disruption of the stem structure. This is consistent with multienzyme (not including RNase ONE) structure mapping

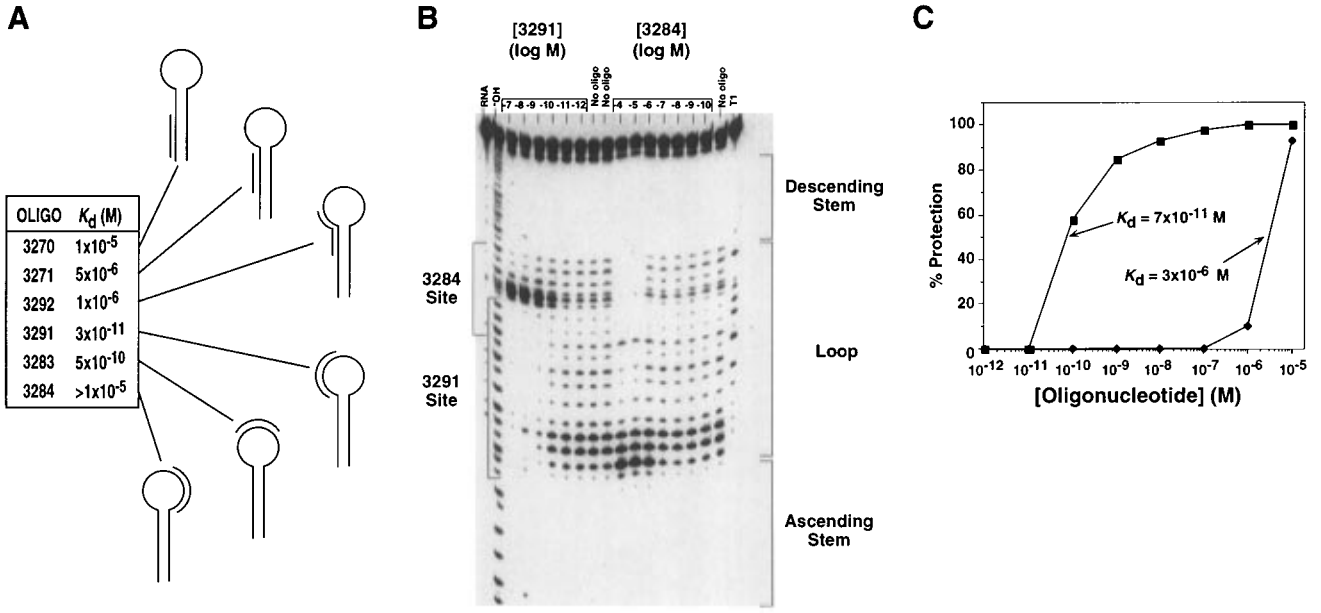

FIGURE 2: (A) Affinities of individual decaribonucleotides for the *ras* stem−loop RNA determined by gel mobility-shift assay. The 5′ → 3′ sequences of the decaribonucleotides are as follows: 3270, CACCACCACC; 3271, GCGCCCACCA; 3292, CGACGGCGCC; 3291, CACACCGACG; 3283, UUGCCCACAC; 3284, CACUCUUGCC. (B) Quantitative RNase ONE footprinting assay of binding of decaribonucleotides to the left (for 3291) and the right (for 3284) sides of the *ras* RNA loop. Primary denaturing PAGE results using 0.5 units of RNase ONE for 5.0 min at ambient temperature are shown. RNA is transcript fragment at the beginning of experiments. No oligo is RNA that has been footprinted in the absence of added antisense oligonucleotide. T1 designates RNA digested with RNase T1. (C) Secondary plot of the primary data in panel B obtained by summing and averaging the band intensities in a given lane at the sequence positions defined by the footprints of panel B as denoted on the left. Squares show data points for 3291 and diamonds show data points for 3284.

of the hybrids (Lima et al., 1992). Footprints of both oligonucleotide titrations do, however, indicate that binding of either one influences the single-strand conformation at adjacent nucleotides of the hybridization site of the other, as evidenced by enhanced intensity nucleolytic cleavage at several nucleotide positions at higher oligonucleotide concentrations. Finally, Figure 2C shows the binding curves generated from the primary data of Figure 2B. The determined values of K_d for both oligonucleotides 3291 and 3284 agree well (±2−3-fold) with the values determined independently by gel mobility-shift assays. The value for 3284 determined by RNase ONE footprinting is probably more accurate, because of the short (minutes) time scale of digestion, than that determined on an hours time scale using gel mobility shift, which results in divergence to artificially lower affinities of kinetically unstable weaker binding interactions (less than or equal to micromolar) (Weeks & Crothers, 1992).

RNase ONE Footprinting of Combinatorial Hybridization Affinity Screening: Library Sequences in Excess of Transcipt. Figure 3 shows the results of RNase ONE footprinting of the interaction of a 10-mer fully sequence-randomized uniform 2′-OMe oligonucleotide library with the 5′-end-labeled *ras* transcript fragment. The 2′-OMe modification was used because it facilitates high-quality automated synthesis of the library and the product obtained is considerably more resistant to chemical and enzymatic degradation than is RNA. Oligonucleotides uniformly substituted with the 2′-OMe modification form hybrids with RNA having helical structure very similar to RNA duplexes (Griffey et al., 1994). Since the hybrids are modestly more stable (Griffey et al., 1994), preferred hybridization of the 3291 sequence as a uniformly substituted 2′-OMe oligonucleotide is probably stoichiometrically limited with a value for K_d <

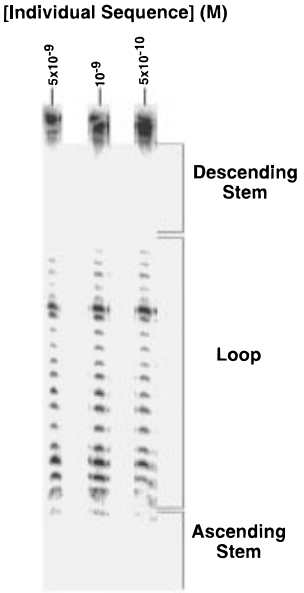

FIGURE 3: RNase ONE footprinting of interaction of a fully sequence-randomized, uniform 2′-OMe substituted decanucleotide library with the *ras* stem−loop. [Individual Sequence] refers to the calculated concentration of each equimolar unique sequence in the library.

3×10^{-11} M (Lima et al., 1992). The concentration of *ras* transcript used likely is close to the true value for the K_d for this oligonucleotide and less than or equal to K_d values for all other oligonucleotides in the library. For the experiment shown in Figure 3, the calculated concentrations of individual sequences in the library in all three lanes are greater, by up to minimally 160-fold, than the estimated highest affinity K_d value and the concentration of transcript. These are the conditions expected to support a footprint for successful hybridization affinity screening by titration of the library

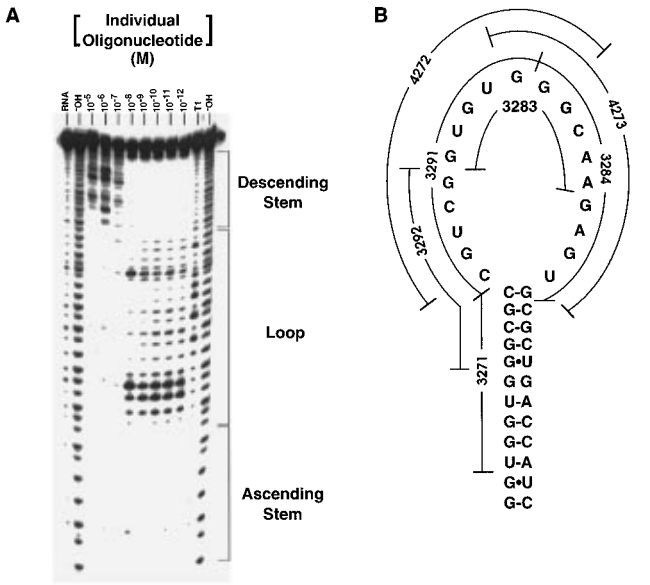

FIGURE 4: (A) RNase ONE footprinting analyzed on denaturing PAGE of the interaction of a mix of seven equimolar decaribonucleotides with *ras* RNA. Notations are as described in previous figures. (B) Sequence-complementary binding sites of the seven decaribonucleotides with respect to the starting *ras* stem−loop structure.

concentration. However, no footprint was observed at any library concentration and there was no apparent melting of the *ras* stem. Attempts to select with even higher concentrations of library than the highest shown (>5 mM) resulted (not shown) in incomplete library solubility, enhanced distortion and smearing of cleavage product bands on denaturing PAGE, and melting of the *ras* stem, without indication of a specific footprint in the loop.

RNase ONE Footprinting of Hybridization of a Seven Oligonucleotide Mix: Sequences in Excess of Transcript. The complexity of the library was reduced to an equimolar mixture of seven representative decaribonucleotides with sequence complementarity to a range of hybridization sites on the *ras* stem−loop (Figure 4B). Unlike the fully randomized library, the oligonucleotide mixture did not contain self-complements of any of the decaribonucleotides. As shown in Figure 4A, at the lower concentrations of individual sequences there is no evidence of footprinting and the stem is intact since both ascending and descending legs are protected from cleavage. By 10^{-7} M, which is about 50-fold lower than the value for the K_d for the 3271 decaribonucleotide, there is partial melting of the stem by strand invasion of 3271, giving protection of the ascending strand of the stem to which it is hybridized and deprotection of the melted and unhybridized descending strand of the stem. However, the footprint that is expected at $\sim 10^{-11}$ M for 3291 is not observed until much higher concentrations, $\sim 10^{-8}$ M. This is within ~10-fold of the concentration of sequences ($\sim 10^{-7}$ M) giving both stem melting and a footprint of the right side of the loop by 3284. From its K_d value, 3284 is not expected to footprint until $\sim 10^{-6}$ M. Thus, there is a shift in apparent binding association constants of *ras* site-specific decaribonucleotides in this seven-sequence mix to substantially lower (for the left side of the loop) or higher (for the right side of the loop and the stem) values than when binding is determined for individual sequences. These results are summarized in Table 1. The net result is an accompanying overall compression of the range of *ras* site hybridization affinities from 10^5-10^6 M to only $10-10^2$ M. Thus, in practice, it is difficult to demonstrate specificity of binding at different sites on the *ras* stem-loop by binding affinity screens based on titrations of the seven-oligonucleotide mix under footprinting conditions.

RNase ONE Footprinting Analysis of Hybridization of Two Oligonucleotide Mixes to ras RNA. The complexity of the library was reduced further to three different component cases of two decaribonucleotides complementary to *ras* RNA (Figure 5). One member of each oligonucleotide pair was 3291, the highest affinity sequence, and the other member was a different sequence complementary to one of three other representative sites with a unique relationship to the *ras* site for 3291. Table 2 shows a summary of the results of RNase ONE footprinting analyses (primary data not shown) of binding titrations of individual and equimolar paired oligonucleotides for each case. The last column of the table shows the direction and the magnitude of the effect of binding of each paired oligonucleotide on binding of 3291 and *vice versa*. Oligonucleotides that bind to the left side of the loop (3291 and 4272) always lose affinity when paired with another oligonucleotide binding to another discontinuous site (3271 or 3284). In contrast, oligonucleotides that bind to the right side of the loop (3284) or the stem (3271) gain affinity when paired with oligonucleotides that bind the left side of the loop. Further, the magnitude of the gain in affinity of one of these oligonucleotides is always matched by an equivalent-magnitude loss of affinity of the paired oligonucleotide. The magnitude of these changes is very minimal for the 3291−3271 pair binding the left side of the loop and the stem and ~10-fold larger for the 3291−3284 pair binding to the left and right sides of the loop. However, the largest magnitude change in affinity is seen for highly overlapping, or site-degenerate, oligonucleotide pairs binding to the left side of the loop (3291−4272). When each oligonucleotide of the pair has the same individual association constant, the change for each when paired at equimolar concentration is to equivalent loss of affinity.

For the three paired oligonucleotide cases, the dependence of the binding isotherm of each decaribonucleotide of the pair on the concentration of the other decaribonucleotide also was determined by RNase ONE footprinting (not shown). Association constants were determined from the midpoints of the binding curves of these experiments. The dependence of these association constants of each oligonucleotide on the concentration of the other oligonucleotide of its pair for each of the three paired cases was then plotted as shown in Figure 6. For case A (Figure 6A), the value for K_a for either oligonucleotide changes only a few-fold as the concentration of the paired oligonucleotide is increased over 5 log units. At 10^{-6} M of either competing oligonucleotide, which is close to the value for K_d for binding of 3271 that disrupts the stem structure, the slightly shifted values for K_a revert back to the values in the absence of the competing oligonucleotide. Thus, the binding affinity of each oligonucleotide of the pair is virtually independent of the binding of the other oligonucleotide over a large range of concentration. For case B (Figure 6B) the values for K_a for each oligonucleotide are not affected by the presence of the other until it reaches $\sim 10^{-9}$ M, or ≥10-fold higher than the individual K_a for either oligonucleotide. Thus, at concentrations that are subsaturating for either oligonucleotide alone, 4272 and 3291 together should additively contribute to the *ras* site-specific

Table 1: *ras* RNA Site-Specific Association Constants for Hybridization of Individual and an Equimolar Mix of Seven Decaribonucleotides[a]

oligo binding site on *ras* RNA	individual oligo K_a[b] (M^{-1})	seven-oligo mix apparent K_a[c] (M^{-1})	K_a ratio[d] (mix/individual)
left side of loop (3291, 4272)	1×10^{10}	1×10^{8}	−100
right side of loop (3284, 4273)	3×10^{5}	1×10^{7}	+33
ascending strand of stem (3271)	2×10^{5}	2×10^{7}	+100

[a] Association constants were determined using the RNase ONE footprinting assay as described in Materials and Methods. Errors in values are estimated ± a factor of 2. [b] Values determined for individual oligoribonucleotides hybridizing to the indicated sites on *ras* RNA. [c] Apparent K_a implies the value observed at the indicated *ras* RNA site by RNase ONE footprinting and may not be the true K_a for any individual oligonucleotide that hybridizes to that site. [d] Values <1.0 or >1.0 are represented as negative or positive whole numbers, respectively, to indicate the magnitude by which they are *decreased* or *increased*, respectively, in the seven-oligonucleotide mix compared to values for individual oligonucleotides binding to the same sites.

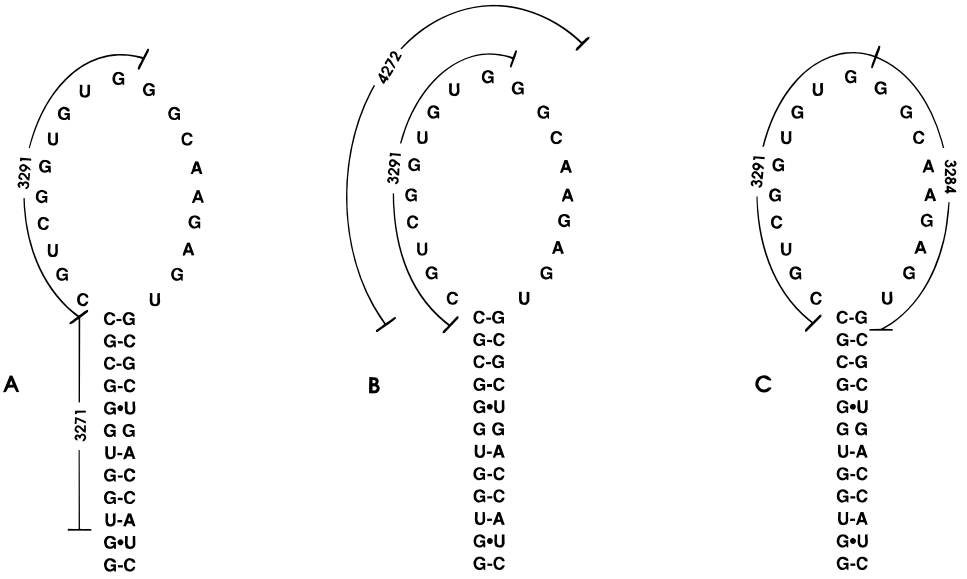

FIGURE 5: *Ras* RNA binding site relationships of three different cases (A−C) of paired antisense oligonucleotides. Each pair includes the highest affinity oligonucleotide, 3291, and one of three other oligonucleotides binding to sites on *ras* RNA with distinctly different relationships to the site for 3291.

Table 2: *ras* RNA Site-Specific Association Constants for Hybridization of Individual and Equimolar Paired Decaribonucleotides[a]

case	first oligo binding site on *ras* RNA	individual first oligo K_a[b] (M^{-1})	first oligo apparent K_a[c] (M^{-1}) with paired oligo	paired oligo	K_a ratio[d] (paired/individual)
A	3291	1×10^{10}	3×10^{9}	3271	−3
A	3271	2×10^{5}	5×10^{5}	3291	+3
B	3291	1×10^{10}	1×10^{8}	4272	−100
B	4272	1×10^{10}	1×10^{8}	3291	−100
C	3291	1×10^{10}	3×10^{8}	3284	−30
C	3284	3×10^{5}	1×10^{7}	3291	+33

[a] Association constants were determined using the RNase ONE footprinting assay as described in Materials and Methods. Errors in values are estimated ± a factor of 2. [b] Values determined for individual oligoribonucleotides hybridizing to *ras* RNA. [c] Apparent K_a implies the value observed at the indicated *ras* RNA site for binding of the first oligonucleotide by RNase ONE footprinting. [d] Values <1.0 or >1.0 are represented as negative or positive whole numbers, respectively, to indicate the magnitude by which they are *decreased* or *increased*, respectively, in the paired oligonucleotide mix compared to values for individual oligonucleotides binding to the same sites.

RNase ONE footprint, which is incapable of distinguishing between these two ligands. At higher concentrations, from 10^{-9} to 10^{-6} M of the second oligonucleotides, the apparent affinities of the first oligonucleotides both decrease by 2 orders of magnitude. Thus, at higher fractional saturation of the left-hand side of the *ras* loop this oligonucleotide pair must become competitive, presumably due to equivalent affinity competition of partially hybridized and unstable intermediates, such that neither oligonucleotide hybridizes completely in preference over the other, thus allowing RNase ONE to more effectively compete for binding. For case C (Figure 6C) there is no change in the apparent K_a values of either oligonucleotide from the individual values until the second oligonucleotide reaches about 10^{-9} M. Thereafter, at every concentration of the second oligonucleotide, the apparent affinity gained by 3284 is exactly matched by affinity lost by 3291. The slopes (+ or −) of these changes in K_a become shallower at 10^{-7} M. The final values for K_a for each oligonucleotide are identical and midway between the two starting high and low values. Together with the appearance, from 10^{-7} to 10^{-6} M of competing ligand, of RNase ONE cleavage of both the ascending and descending strands of the *ras* stem (primary gel data not shown), this indicates affinities for either oligonucleotide for the unfolded *ras* sequence are indistinguishable by footprinting. This confirms that the ~10^6-fold difference in association constant values measured for individual oligonucleotides is entirely due to the structure of the *ras* stem−loop.

RNase ONE Footprinting, Post Gel Mobility-Shift Resolution, of Combinatorial Hybridization Affinity Screening:

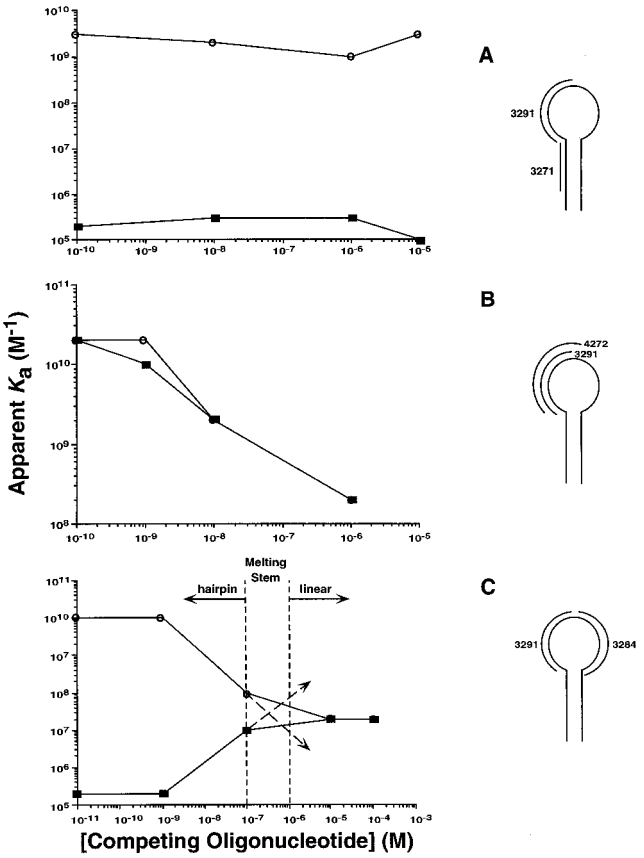

FIGURE 6: Dependence of equilibrium binding association constants of each decaribonucleotide on the concentration of the other competing oligonucleotide for each of the three paired oligonucleotide cases. Data are replotted from primary binding isotherm plots (not shown). For each data point the titrated oligonucleotide was varied over 10^{-11} to 10^{-5} M, 5′-end-labeled *ras* RNA was held constant at 1−5 pM, the second (competing) oligonucleotide was held constant at the indicated concentration, and binding constants were determined from the midpoints of the primary binding curves. Apparent K_a denotes the *ras* RNA site-specific values determined by RNase ONE footprinting, which may not be the true K_a values for the individual oligonucleotides. Open circles are data points for 3291 and solid squares are data points for the other oligonucleotide of each pair. Competing oligonucleotide here applies in the operational sense in experimental design and does not mean to imply kinetically formal relationships of paired oligonucleotides. A presumed systematic error for experiments titrating 3291 in case A resulted in values for apparent K_a that are ≤ 10-fold lower than for most other determinations, but this does not affect the change in values with varied concentration of 3284.

Transcipt in Excess of Library Sequences. Experiments were performed as described in Materials and Methods and representative results are shown in Figure 7. The outside lanes, especially the far right lane, are greatly overloaded compared to the three inside lanes (Figure 7A). The far right lane is for free labeled transcript only, which can be recovered in abundance from mobility-shift gels. Similarly, for the far left lane there was little or no bound transcript detected on gel mobility shift and it is evident that primarily excess free transcript was recovered from native gel slices and loaded on denaturing PAGE. For these two overloaded lanes, nonenzymatic and nonspecific background degradation of the labeled *ras* RNA, after the many manipulations of the experimental procedure, is readily evident. Since the major portion of material is still full-length transcript, degradation must be primarily by single hit kinetics with a bias toward larger fragments at the top of the gel. For the

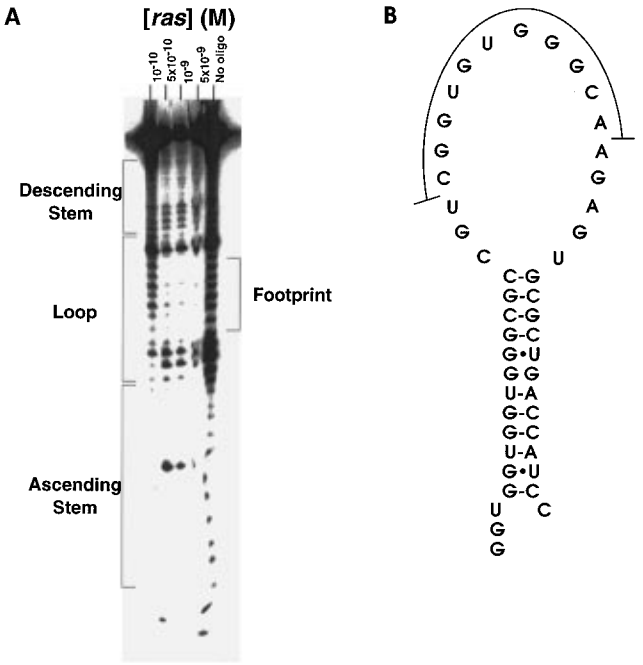

FIGURE 7: (A) Denaturing PAGE analysis of RNase ONE footprinting in crushed gel slices, post gel mobility-shift resolution, of 1:1 stoichiometry *ras* RNA·2′-OMe decanucleotide complexes formed in hybridization affinity screens using transcript in excess over individual library sequences. Fully sequence-randomized uniform 2′-OMe-substituted library was held constant for a calculated concentration of individual library sequences of 100 pM. (B) Schematic representation of the sequence positions of the footprint on *ras* RNA.

inside lanes covering RNA concentrations from 5×10^{-10} to 5×10^{-9} M, bound complexes were observed on mobility-shift gels and the recovered material is limiting and relatively underloaded on denaturing PAGE. There is a clearly titrated RNase ONE footprint within the loop of these complexes that must be accounted for by preferential binding of the library oligonucleotides to nondegraded loop sequences and subsequent RNase ONE cleavage flanking the oligonucleotide(s) binding site(s). The cleavage of 5′- and 3′-most loop sequences must be due to RNase ONE because formation of products is in excess of background cleavage outside of the loop.

The span of the footprint is shifted 3 nt 3′ of the binding site for 3291 (Figure 7B). There are several contributing explanations consistent with this result. First, the footprint for 3291 is longer than the binding site by 2−3 nt on the 3′-side as described earlier (Figure 2). Second, the first three single-nucleotide 3′-shifted 10-mer oligonucleotides binding the 5′-most side of the loop—3291, 4272, and one other (data not shown)—have equivalent affinity and this defines a single 12-nt, not a 10-nt, highest affinity 5′-loop site. Third, oligonucleotide 3283 binds to the top of the loop only 10-fold less tightly than these three isoenergetic oligonucleotides and discrimination would require a demanding screen. Fourth, the binding affinity screening conditions, in fact, are nonideal, with the concentration of individual library sequences only 5−50-fold less than that of labeled *ras* RNA, due to limitations on detection of 1:1 stoichiometry bound complexes. However, the highest *ras* RNA concentration of 5×10^{-9} M is ≥10-fold greater than the K_d for 3291 (2′-OMe and RNA oligonucleotides have roughly similar affinities (Griffey et al., 1994)) and a footprint reflective of the expected ≥90% bound transcript is observed. This result

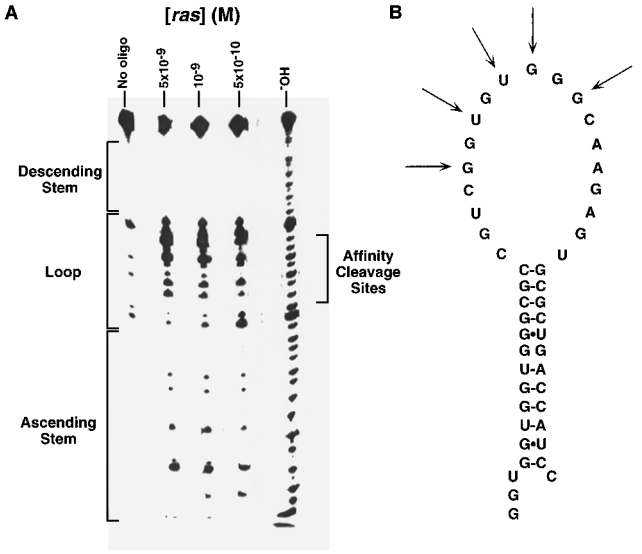

FIGURE 8: (A) Denaturing PAGE analysis of RNase H cleavage in solution of 1:1 stoichiometry *ras* RNA·DNA decanucleotide complexes formed in hybridization affinity screens using transcript in large excess over individual library sequences. Fully sequence randomized DNA library was held constant for a calculated concentration of individual library sequences of 100 pM. (B) Schematic representation of the sequence positions of RNase H cleavage. Although affinity cleavage is indicated over the entire left side of the *ras* loop (panel A), only sequence positions of cleavage significantly above background degradation are indicated in panel B.

is also important because it demonstrates that the predicted presence of equimolar self-complements for every *ras*−RNA binding oligonucleotide in the fully randomized library does not greatly inhibit selection for binding to excess *ras* transcript. Self-complements may, however, lower the concentration of oligonucleotide·*ras* complexes and make detection more difficult. Fifth, it was reported previously (Lima et al., 1992) that highest affinity oligonucleotides cause the smallest change in *ras* RNA conformation with the resultant smallest difference in migrational retardation on mobility-shift gels compared to free *ras*: only 2 mm for 3291 and 5 mm for 3283 *vs* 12 mm for 3284. Thus, in initially removing the large excess of free *ras* RNA from mobility-shift gels it is difficult not to also remove some of the closely adjacent left side of the loop binding oligonucleotide·*ras* complexes and in attempting to subsequently specifically recover the latter it is difficult to not recover some of the top of the loop binding oligonucleotide·*ras* complexes. When all these factors are considered, the RNase ONE footprinting results are in accord with the best that should be expected for a successful combinatorial binding affinity screen and this mode of analysis.

RNase H Cleavage Assay of Combinatorial Hybridization Affinity Screening: Transcript in Excess of Library Sequences. Experiments were performed as described in Materials and Methods and typical results are shown in Figure 8. In general, the results are superior to those shown in Figure 7. With fewer manipulations, due to RNase H treatment in the combinatorial hybridization affinity screening solution following equilibration, the level of spontaneous background degradation is greatly reduced (far left lane of Figure 8A). Further, it is limited to the loop nucleotides, consistent with access of single-strand, but not double-strand, sequence positions to an in-line stereochemistry of RNA 2′-OH and 5′-OR groups at sites of phosphodiester hydrolysis. The most reactive sequence positions are also the most reactive in the presence of added specific base (far right lane). The complete absence of cleavage products of the descending strand of the *ras* RNA stem for all experiments indicates that RNase H cleavage has been restricted to sequences of sites of formation of RNA·DNA heteroduplexes with the *ras* loop only. Low molecular weight cleavage products of lower yield than for products of primary cleavage of loop heteroduplexes must then be due to overdigestion with RNase H and some secondary cleavage events, not due to primary cleavage of the ascending strand of the *ras* stem. The results of these experiments are also superior because it was possible to achieve more preferred screening conditions. Since DNA oligonucleotides required for RNase H activity have significantly lower affinity for target RNA than either RNA or 2′-OMe oligonucleotides (Griffey et al., 1994), detection limit constraints can be met for complexes at concentrations that are 50−500-fold below the lowest K_d for DNA·RNA heteroduplexes with the left side of the *ras* loop. This is a 10-fold improvement over the difference between complex concentration and the lower K_d for RNA or 2′-OMe oligonucleotides (Figure 7).

As for the RNase ONE footprinting experiments of Figure 7, the sequence positions of RNase H cleavage of the loop are 3′-shifted (Figure 8B). Some of the reasons are probably the same: the highest affinity isoenergetic 5′-loop site is 12 nt and the top of the loop site binds only 10-fold less well. However, in addition, it has been shown (Crooke et al., 1995) that sequence positions of RNase H cleavage are 3′-shifted with respect to the RNA target. Finally, although RNase H does not show base specificity it does have some ill-defined helix conformational specificity and is subject to steric constraints imposed by the target structure and so does not cleave equally well at all heteroduplex sequence positions (Figure 8A). Therefore, it probably would be misleading to assume a strict correspondence of greatest yield of products for RNase H cleavage at the top of the loop with highest concentration of oligonucleotide complexes with the top of the loop.

DISCUSSION

Combinatorial Hybridization Affinity Screening in Solution. Our overall goal has been to explore strategies for equilibrium binding affinity-based screening, performed *in vitro*, in solution, under quasiphysiologic conditions (*i.e.*, pH, temperature, salt species, and concentration), of combinatorial oligonucleotide libraries against defined RNA targets. We view this as an accessible approach for the identification of preferred hybridization sites, which is the first step toward *in vitro* optimization of antisense oligonucleotide·folded RNA recognition (Lima et al., 1996). For reasons we have discussed earlier and have developed more fully elsewhere (Lima et al., 1996), this may have value for predicting and improving biological potency and specificity of antisense inhibition. We wanted to avoid screening on solid supports or employing physical separation, because of the potential for the introduction of bias and in order to minimize the number of manipulations required.

Library Design. We chose to use short (10-mer) oligonucleotide libraries in order to restrict the library complexity (calculated as $4^{10} = 1\ 048\ 576$ sequences) so that all possible sequences could be synthesized with equimolar base repre-

sentation at each sequence position and in equivalent and adequate amounts (Davis & Ecker, 1996). Thus, a single 10-mer oligonucleotide synthesis yields sufficient fully randomized library for many searches for preferred sites of 10-mer hybridization on RNAs of any sequence. Short oligonucleotide libraries also avoid a bias for suboptimal recognition of RNA structure that generally is the case for screens using long (20-mer) oligonucleotides, as was discussed earlier (Woolf et al., 1992; Stein & Krieg, 1994; Wagner, 1994). Further, the heteroduplex affinity at the identified, preferred sites falls within the operational range of measurement of readily accessible binding assays, in order to facilitate subsequent quantitative characterization and eventual oligonucleotide optimization of affinity and specificity (Lima et al., 1996). Importantly, the stability of intramolecular interactions (*i.e.*, stem−loops) of short library sequences is attenuated. Those short library oligonucleotides that do have stable internal structure will have diminished affinity of hybridization with RNA (Chastain & Tinoco, 1993; Freier, 1993) and should not be chosen in affinity-based screens. Unlike libraries of some other nucleic acid screening strategies, the libraries used in this strategy have no internal fixed sequence positions (Ecker et al., 1993) or external conserved flanking sequences (Ellington & Szostak, 1990; Robertson & Joyce, 1990; Tuerk & Gold, 1990), which would be expected to limit and/or bias screens for binding to folded RNA.

Individual Oligonucleotide Hybridization to ras RNA. The data presented in Figure 2A for the binding affinities determined by gel mobility-shift assays of six different decaribonucleotides with sequences complementary to a range of possible hybridization sites on the mutant Ha-*ras* mRNA 47-nt fragment (Figure 1) confirm that this RNA should be particularly well-suited as a model target for exploring combinatorial oligonucleotide hybridization affinity screening. It is a representative member of the ubiquitous stem−loop structures found in folded RNA and it is small enough to be readily synthesized and for oligonucleotide binding to be easily characterized. Further, there is a relatively large loop of 19 single-strand nucleotides devoid of other complicating secondary structure elements, such as divergent stems or involvement in pseudoknots, which is attractive as an element for antisense oligonucleotide hybridization. In fact, it is observed that 10-mer oligonucleotides bind the 5′-most side of the loop exceptionally well (Figure 2A) (Lima et al., 1992). Perhaps of most importance for a paradigm model study, the very large 10^5-10^6 M range of dissociation constants for decaribonucleotides hybridizing to different sites on *ras* RNA is a result that would seem to favor binding that is specific for the 5′-loop in preference over binding to other *ras* RNA sites in affinity-based screens of carefully titrated concentrations of combinatorial oligonucleotide libraries.

RNase ONE Footprinting Assay. The gel mobility-shift assay is not suitable for combinatorial hybridization affinity screening, because it is not possible to readily discriminate between binding of different length-matched oligonucleotides of a pool to different sites on *ras* RNA (Lima et al., 1992). An appropriate enzymatic footprinting assay should not be subject to this constraint. Therefore, we have demonstrated that RNase ONE (Promega) is exceptionally useful for the footprinting analysis of oligonucleotide hybridization to *ras* RNA. RNase ONE is a single-strand specific and nucleotide base-independent endoribonuclease that cleaves at all sequence positions, including to within 1−3 nt from the end(s) of heteroduplexes formed with oligonucleotides of diverse backbone substitution chemistries, which are completely immune to cleavage. Therefore, very high contrast and tightly demarcated footprints of *ras* site-specific binding of oligonucleotides are obtained (Figure 2B). This assay is additionally useful for providing information about changes in *ras* RNA secondary structure and loop conformation upon oligonucleotide binding, from the appearance or disappearance of cleavable nucleotides and from enhanced or diminished relative yield of products at cleaved nucleotides (Figure 2B). Further, values for thermodynamic equilibrium binding constants for oligonucleotide hybridization to *ras* RNA are essentially identical when determined by either the gel mobility-shift or RNase ONE footprinting assays (Figure 2C), with the latter considered to be more accurate for weak binding oligonucleotides (for reasons discussed earlier). Finally, detection of an RNase ONE footprint requires that the concentration of the hybridizing oligonucleotide should at least approach both the K_d for its interaction with *ras* RNA, in order to obtain binding, and the concentration of the *ras* RNA, in order to protect a sizeable fraction of total RNA from digestion. These requirements are consistent with a prominent stated goal of screening in solution of pooled combinatorial libraries of any composition (Pinilla et al., 1995): each unique compound of the library should be screened at a concentration that will allow a single active one to register a response in *in vitro* binding assays or bioassays, generally requiring significant fractional saturation of the binding site of the molecular target. This suggested that the footprinting assay format may be appropriate for hybridization affinity screening of combinatorial oligonucleotide libraries.

Unsuccessful Combinatorial Screening for Hybridization. Using a fully sequence-randomized 10-mer oligonucleotide library, at concentrations that were below those leading to artifacts attributable to insolubility and high ionic strength, it was not possible to accrue evidence for an RNase ONE footprint indicative of selective oligonucleotide binding to any site on *ras* RNA (Figure 3). One likely factor contributing to this failure is the theoretical presence of equimolar self-complements of every oligonucleotide having sequence complementarity with a site on *ras* RNA. Hybridization of *ras* RNA binding oligonucleotides to self-complements will lower their effective concentration and may be expected to drive the observed concentration of library which gives sufficient oligonucleotide binding to *ras* RNA in order to detect a footprint to a higher concentration than would be expected in the absence of self-complement(s). However, this explanation may not be sufficient to account for the complete absence of a footprint. The 5′-most side of the *ras* loop binds complementary oligonucleotides with stoichiometrically limited observed association affinity constants severalfold higher than for length-matched complement binding of those oligonucleotides (Lima et al., 1992). Further, the calculated concentration of library oligonucleotides was greater than 2 orders of magnitude above the observed dissociation binding constant for binding of individual oligonucleotides to this preferred site on *ras* RNA. If no other processes were involved, these factors would tend to favor binding of oligonucleotide(s) to the 5′-loop.

Reduced Complexity Component Systems. In order to better ascertain the importance of oligonucleotide library self-complements and to begin to understand what, if any, other phenomena may emerge with pooled oligonucleotides, experiments were performed using a mixture of seven equimolar decaribonucleotides complementary to a range of sites on *ras* RNA, wherein none were complements of any of the others (Figure 4B). The results of titration experiments using the RNase ONE footprinting assay are shown in Figure 4A and the determined *ras* RNA site-specific binding constants are summarized in Table 1. Reducing the complexity of the oligonucleotide mixture in this way provides for a footprint of loop nucleotides, suggesting that removing the possibility of self-complement hybridization of oligonucleotides complementary to *ras* RNA is at least a partial solution to the problem. However, all of the *ras* RNA site-specific apparent association constants for the mix are significantly different than for binding of individual oligonucleotides. Cumulatively, these are observed to result in a leveling effect on *ras* RNA binding site discrimination, with the highest and lowest affinity sites for individual oligonucleotides moving in the mix to lower and higher affinity, respectively, and loop binding occuring almost concomitantly with stem melting. These results strongly suggest that processes other than self-complement hybridization also must be at work.

The complexity was reduced further to a minimal multiplicity of two oligonucleotides from the fully randomized library in order to dissect out and understand the simplest processes resulting from the interplay of multiple oligonucleotides with *ras* RNA, which must operate together in higher complexity mixes. Since the goal of hybridization affinity screens with *ras* RNA is to demonstrate selective binding at the 5′-loop site, oligonucleotide 3291 was included as one member of each of three oligonucleotide pairs (Figure 5), with the second oligonucleotide complementary to the ascending strand of the stem (case A), overlapping with 3291 at the 5′-loop site (case B), or complementary to the 3′-loop site (case C). These binding interactions were characterized by equimolar binding titrations of the paired oligonucleotides (Table 2), binding titrations of one oligonucleotide in the presence of different fixed concentrations of the other for determinations of the dependence of values for association binding constants of one oligonucleotide on the concentration of the other (Figure 6), and determinations of association and dissociation rate constants.

The accumulated thermodynamic, kinetic, and structural data obtained by RNase ONE footprinting and gel mobility-shift experiments for the three paired oligonucleotide cases was used to construct the binding schemes depicted in Figure 9. These mechanisms pertain to the relatively large oligonucleotide concentration range from $\sim 10^{-9}$ to $\sim 10^{-6}$ M. The former value is the lowest for which deviations from individual K_as are seen for paired oligonucleotides and the latter value is at the upper limit for retention of (at least partial) *ras* RNA secondary structure (Figure 6). Above and below these concentrations the binding behaviors may deviate from the constructs of Figure 9 (especially for cases B and C). Since the thermodynamic and kinetic constants are dependent on the relative concentrations of the paired oligonucleotides (Figure 6), all three schemes were determined for when the paired oligonucleotides are equimolar, as they would be in the fully randomized oligonucleotide library. We assume that the binary complexes shown for cases A and C lie on productive pathways to ternary complexes, as depicted. Attempts to prove this, and to independently obtain values for rate and equilibrium constants, by using pulse−chase isotope trapping technology (Rose, 1980), were not successful, because the requirements for these experiments were not compatible with formation of discrete complexes but resulted in the formation of aggregates (results not shown).

For all three paired oligonucleotide cases the data for binding events along the edges of the schemes shown in Figure 9 fit well to established kinetic mechanism formalisms (Klotz, 1986). Thus, for case A, where the two oligonucleotide binding sites are nonoverlapping, $K_1 = K_2$ (±3-fold) for the same oligonucleotide and, therefore, the site affinities are essentially independent and fixed. There is an allowed random, sequential binding order, but inspection of K and k values for both oligonucleotides indicates that when they are equimolar the upper pathway is preferred and binding is ordered, sequential. For case B, the binding sites are mutually exclusive and values for K and k are the same for each oligonucleotide, so that when they are equimolar binding is competitive and neither pathway is preferred over the other. Since the values for K for each oligonucleotide in the presence of the other are less than for the individual oligonucleotides, the sites may be characterized as dependent and changing. For case C, the sites are not competitive, but for either oligonucleotide $K_1 \neq K_2$ in the absence and presence, respectively, of the other and so the sites are dependent and changing; in fact, they are mutually allosteric. Formally, binding of 3291 gives positive heterotropic cooperative facilitation of binding of 3284, and binding of 3284 shows negative heterotropic cooperative inhibition of binding of 3291. Although there is an allowed random, sequential binding order, inspection of K and k values for both oligonucleotides reveals that when they are equimolar the upper pathway is preferred and binding is approximately ordered, sequential.

Even though close inspection of the kinetic mechanisms of Figure 9 can allow discrimination between allowed and preferred pathways (as above), this is not the best way to appreciate concentration-dependent binding to different functional classes of *ras* RNA sites of individual compared to paired oligonucleotides. Accordingly, as a preferred formalism, Figure 10 shows *ras* RNA site-specific free energies of binding at three concentrations for each of the individual and equimolar paired oligonucleotide combinations. Although transition-state free energy levels in going from individual to paired oligonucleotides were not determined, the kinetic barriers should be of the same magnitude as for individual oligonucleotide binding, because there is no problem reaching equilibrium binding under the same conditions. Further, in this study it is the relationships of ground-state free energies of oligonucleotide binding at equilibrium that determine the success or failure of binding affinity titration screens.

Viewed in this perspective, it is seen that for all three cases the largest changes in free energies of ground states over the range of concentrations shown is observed for the starting states. For cases A and C the binding of 3291 is always of lowest energy for the individual oligonucleotide or when equimolar with the other over the range from 10^{-11} to 10^{-7}

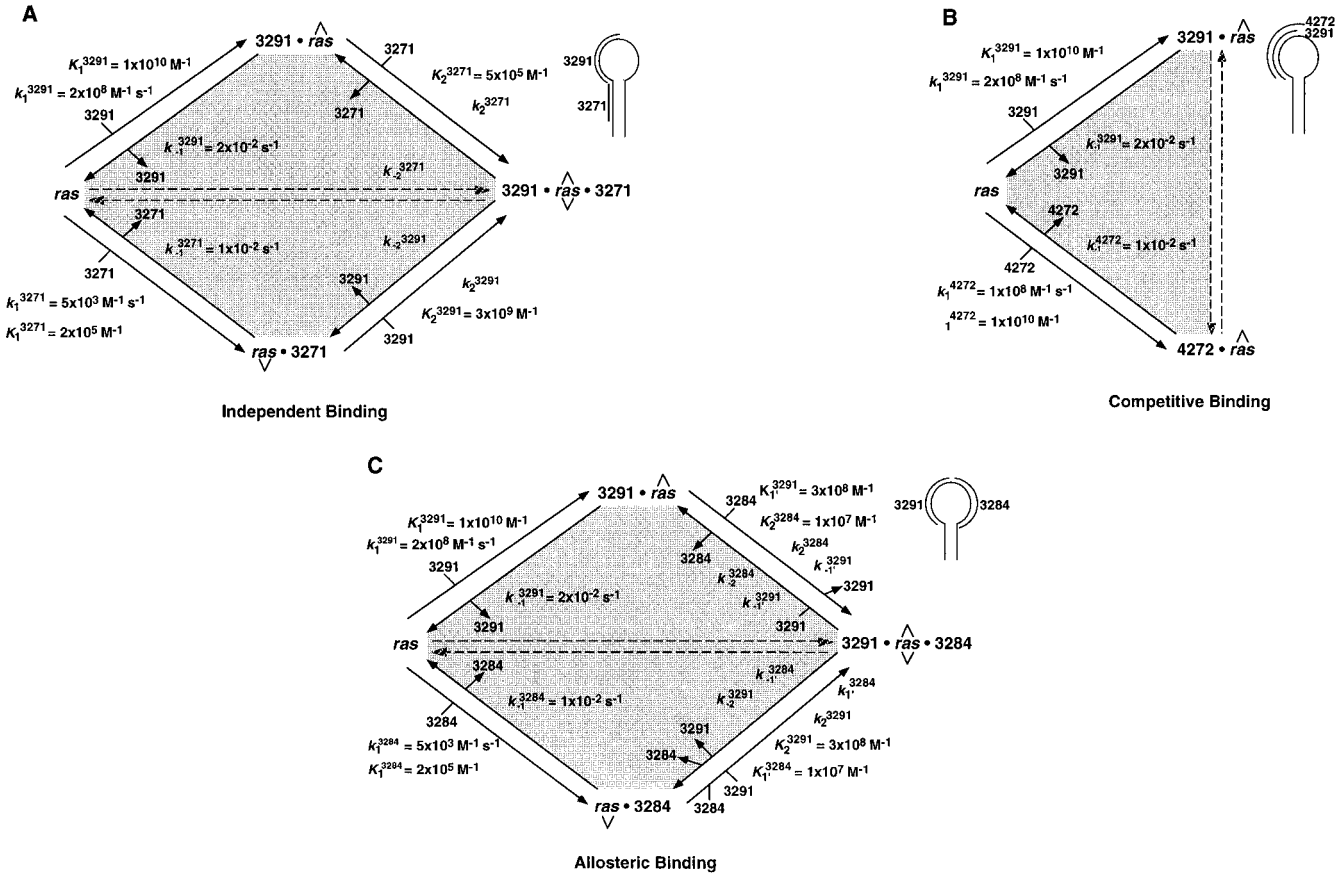

FIGURE 9: *Ras* RNA site-specific kinetic schemes for binding of the three different two-decaribonucleotide combinations. Edge pathways (solid arrows) denote individual and sequential equilibrium binding events involving only fully hybridized complexes, for which site-specific and ligand-specific parameters are the same (Klotz, 1986). (A) Binding at nonoverlapping sites with an allowed random, sequential binding order and independent and fixed site affinities: independent sites. (B) Mutually exclusive binding at overlapping sites with dependent and changing site affinities: competitive sites. (C) Binding at nonoverlapping sites with an allowed random, sequential binding order and mutually dependent and changing site affinities: allosteric sites. Internal, shaded surfaces represent alternative binding pathways involving partially hybridized intermediates and dashed arrows represent concerted binding pathways. Oligonucleotides binding to the left or right sides of the *ras* loop are shown to the left or right of *ras* in notation for complexes. Noncovalent complexes are designated by solid circles between *ras* and ligands, and *ras* species with different secondary and/or conformational structure than free *ras* (no notation) are denoted using superscript carets or subscript inverted carets or both. K_1 and K_2 are site-specific association constants for first oligonucleotide binding in the absence and second oligonucleotide binding in the presence of the other oligonucleotide, respectively. k_1 and k_2 are association rate constants of first and second bound oligonucleotides, and k_{-1} and k_{-2} are dissociation rate constants for first and second bound oligonucleotides. $K_{1'}$ are induced association constants for the oligonucleotide at the first bound site caused by binding of the other oligonucleotide at the second bound site, and $k_{1'}$ and $k_{-1'}$ are induced association and dissociation rate constants at the first bound site caused by binding of the other oligonucleotide at the second bound site. Values for all constants were determined for the equimolar oligonucleotide pairs. All thermodynamic association constant values shown are from RNase ONE footprinting, but most also were determined by gel mobility-shift assays with good agreement (±2−3-fold) except for the lowest affinity oligonucleotides, for which the footprinting values are considered more accurate (see Materials and Methods). Dissociation rate constants were determined by gel mobility-shift assays and bimolecular association rate constants were calculated from the measured dissociation rates and equilibrium constants ($K_a = k_n/k_{-n}$). Some association rates also were measured directly by the gel mobility-shift assay and were in close agreement with calculated values (±2-fold). Rate constant values for second oligonucleotide binding of either pathway for cases A and C were not determined.

M. For case C the energy difference between the 3291 site and the 3284 site in the paired situation is always significantly less than the difference for the individual oligonucleotides at all concentrations. The energies at the 3291 site and the 3284 site are equivalent when both oligonucleotides are present at 10^{-5} M. In contrast, for case A the change in the energy difference between the 3291 and 3271 sites when the oligonucleotides are paired or alone is minimal and it is nearly constant over the full range of oligonucleotide concentration. For case B the 3291 and 4272 site are highly degenerate and have the same energies at all concentrations for individual and paired situations, but the energies for the paired oligonucleotides are always significantly higher than for oligonucleotides measured independently. Clearly, case A represents the only site relationship where it is possible to move the energy of the starting state (*i.e.*, by titration) above that for the 3291 site while maintaining it far enough below the energy for the 3271 site to achieve preferential 5′-loop site binding discrimination. For cases B and C the energies of both sites when the oligonucleotides are paired are either the same (case B) or so close (case C) that there is no way to situate the starting state energy by changing oligonucleotide concentration to favor binding at the 3291 site over the other.

Reconstruction of Events with Full-Complexity Libraries. From the above reductionistic analyses it becomes possible to attempt to account for the failure of hybridization affinity screening of full-complexity oligonucleotide libraries under enzymatic footprinting conditions when all of the indpendently identified different binding interactions operate simultaneously. Competition of binding of oligonucleotides to self-complements *vs* to *ras* RNA will tend to drive titrations

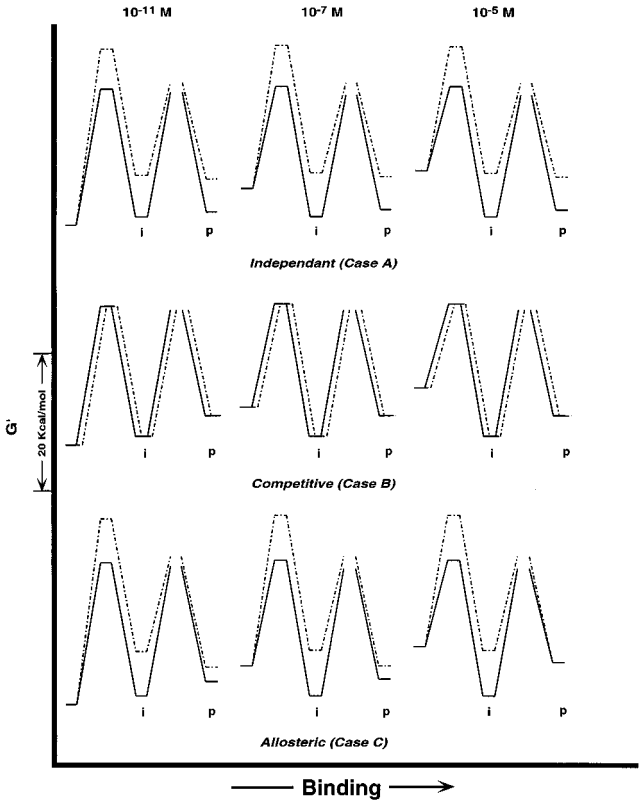

FIGURE 10: Site-specific energetics of binding interactions of *ras* RNA with the three combinations of two equimolar decaribonucleotides. The edge mechanisms of Figure 9 are assumed. G′ is the biochemical free energy under our experimental conditions. Ground-state values of G′ were calculated from both equilibrium and rate constants and transition state values for G′ were calculated from association and dissociation rate constants according to standard equations (Klotz, 1986; Stenesh, 1993). The values of 10^{-11} and 10^{-7} M delimit the concentration range giving the largest perturbations in K_a values for paired oligonucleotides compared to for individual oligonucleotides, with the imposed constraint of retention of *ras* RNA secondary structure. The free energy diagram for any other concentration falling between these two values would simply be an interpolation of the diagrams for these limit values. The high value of 10^{-5} M is included in order to show the change in energetics upon melting of the *ras* RNA secondary structure (*i.e.*, as in cases A and C). For all three cases, the solid line represents the energetics of binding of 3291 to the left side of the *ras* loop and the broken line represents the energetics of binding of the other oligonucleotide in each pair with its respective site on *ras* RNA. The starting ground-state free energy for each diagram is the same value, by convention, for free *ras* RNA and 3291 or free *ras* RNA and the other oligonucleotide. Bound species represent fully hybridized complexes; no attempt is made to show partially hybridized intermediates. The first bound intermediate energies are for binary complexes of *ras* RNA and 3291 or *ras* RNA and the other oligonucleotide alone (i). The second bound complex energies are for the interaction of *ras* RNA and 3291 only or for *ras* RNA and the other oligonucleotide only when both 3291 and the other oligonucleotide are paired (p); *i.e.*, they are *ras* RNA site-specific binding energies and do not represent total energies of ternary complexes.

to higher library concentrations in order to detect the latter. Competitive binding of sequence-degenerate oligonucleotides for the 5′-side of the *ras* loop will depress higher fractional saturation binding needed for a good footprint and require even higher concentrations of library. At the same time, allosteric interaction of oligonucleotides complementary to the 5′- and 3′-sides of the loop will drive the affinity for the 5′-side down and necessitate yet higher library concentrations for binding. The affinity for the 3′-side will be pushed upward so that it will not be possible to obtain complete protection of the 5′-side without also some binding to the 3′-side. Further, since complete hybridization of oligonucleotides to both the 3′- and 5′-sides of the loop is topologically impossible with retention of the stem−loop secondary structure, at a high enough library concentration the stem will melt before there can be saturation binding of the 5′-loop site. When this happens all oligonucleotides complementary to *ras* RNA sequences bind with only minor sequence-dependent differences in affinity and all possibility of discrimination based on target RNA structure is lost. Finally, all these processes are expected to be greatly exacerbated by the much larger number of oligonucleotides that are sequence-degenerate with the selected ones studied above, with the result that all of the described effects probably happen at the same library concentration.

Control of Complexity Constraints. The present study acutely illustrates the limitations of current formal understanding and treatment of both theory and experiment dealing with binding of pooled combinatorial libraries with defined molecular targets in solution. Construction of formal kinetic binding schemes (analogous to Figure 9) and derivation of accompanying mathematical descriptions are only possible when the identities of all interacting species and the kinetic and thermodynamic parameters describing all complexes formed are known. For very complex systems, it is impractical to independently determine all of these experimentally, and whereas attempts have been made in special cases to calculate binding affinities of all complexes using computers (Freier et al., 1995), as we have shown here, ideal binding behavior cannot be assumed when all components are present together. Mathematical descriptions of numerous component systems can be corrected to a degree for nonideal bulk effects (*i.e.*, solvent, salt, etc.) by the use of activity coefficients (Wyman & Gill, 1990), but this treatment does not begin to address the kinds of ligand interdependencies we have identified.

As a consequence of both the goals and methods of syntheses, solution-based screening of pooled and unbiased combinatorial libraries is faced with the unique situation of selecting from large to enormous numbers of compounds of equivalent representation composed of groupings of many closely related molecules of shared functionality, or quasispecies (Eigen, 1992). Every quasispecies is related to others and together they comprise a seamless continuum (quasispecies of quasispecies) covering the total chemical diversity of the pool. It may be especially challenging to identify single active structures because any given one should have many close relatives at the same molarity; the more chemically diverse the mix the more different molecules with close relatives will be present, and the larger the number of distinct structures the more seamless will be the relations between any given group and others. This certainly is true in the present work for the randomized oligonucleotide libraries. The relations of different oligonucleotide hybridization sites on *ras* RNA also are not discontinuous. Thus, it would appear that structurally degenerate complexity and multiple linked interactions (Wyman & Gill, 1990) are the defining issues for binding affinity-based screening of unbiased combinatorial pools of molecules.

In applications, such as the present study, requiring full-complexity, unbiased libraries, the only solution is the elimination of all potential linked binding interactions in a

way that preserves massive coparallel screening only of every possible independent bimolecular (*i.e.*, library oligonucleotide·RNA) binding event.[2] This requires that the concentration of oligonucleotide library be held such that the calculated concentration of individual library sequence is limiting and significantly less than the K_d for the highest affinity bimolecular complex(es) with the target RNA. Complex formation will then be controlled solely by the concentration of the RNA, which can be titrated around this K_d value in order to preferentially select for tightest interactions. Intermolecular interactions among self-complementary library sequences will be strongly disfavored and the only statistically significant population of bound complexes will have 1:1 stoichiometry and so all library oligonucleotide·RNA interactions should behave as if measured independently and there should be no "melting-out" of individual RNA molecules.

Successful Combinatorial Screening for Hybridization. The above requirements were approximated in the experiments of Figure 7 and were met for the experiments of Figure 8 utilizing fully randomized 10-mer oligonucleotide libraries. As discussed in the Results section, both experiments demonstrated preferential hybridization to the 5′-most and top nucleotides of the *ras* RNA loop. The better results observed for experiments of Figure 8 can be attributed to better adherence to the screening requirements, the use of a simpler assay requiring fewer manipulations, and a surprising signal amplification effect (Lima et al., 1997). The purpose for performing the experiments of Figure 7 was to show that the RNase ONE footprinting assay can accurately report on preferred site binding to *ras* RNA of oligonucleotides of complex combinatorial libraries when binding is achieved under the correct screening conditions. However, it is clear that the requirements for footprinting (reviewed earlier) are mutually exclusive with the screening requirements without the intervention of a cumbersome physical separation step to resolve the small amount of oligonucleotide·*ras* RNA heteroduplexes from the much larger amount of free *ras* RNA. Therefore, selective cleavage of heteroduplexed DNA oligonucleotide·RNA sites on *ras* RNA by RNase H in solution, immediately following library hybridization equilibrium, is the simpler and preferred assay. Since affinity cleavage patterns on gels are the sum of all patterns for individual bimolecular complexes, including those that are sequence-overlapping, this assay can identify preferred hybridization sites on RNA that are longer than the (10-mer) library oligonucleotides (as in Figure 8).

Toward Rational Optimization of Antisense Oligonucleotides. By adhering to the optimal screening requirements established in this study and using the RNase H cleavage assay, we recently have been able to use combinatorial 10-mer DNA oligonucleotide hybridization affinity screening in solution to correctly identify sites of preferred hybridization of antisense oligonucleotides in the 5′-440 nt of hepatitis C virus RNA. Subsequent optimization of exact sequence, length, and backbone chemical composition of oligonucleotides complementary to these identified sites for enhanced *in vitro* binding affinity and specificity resulted in antisense that was more biologically potent and selective in *in vitro* translation and cell-based expression assays than were identical chemical composition 20-mer oligonucleotides chosen by traditional transcript sequence walks (Lima et al., 1997). Thus, it is likely that this *in vitro* approach may be applied to other RNAs to successfully predict antisense oligonucleotide inhibitory activities in biological assays.

Significance and Implications for Combinatorial Biology and Chemistry. First, it is likely that nature employs limited diversity combinatorial intra- and intermolecular hybridization interactions, replete with the features of competitive and allosteric binding, secondary structure and conformational changes, and fine tuning of energetics, for the functional regulation of numerous nucleic acids (Emerick & Woodson, 1994; LaGrandeur et al., 1994; Lingner et al., 1994). It should even be possible to mimic these regulatory elements for practical applications (Porta & Lizardi, 1995).

Second, a question with broader impact is, do any of the behaviors observed for interactions of nucleic acid libraries with RNA have any relevance to the much larger world of small molecule combinatorial library interactions with biomolecules, especially proteins? In comparison to study of the latter, the kinds of reductionistic binding analyses performed here were greatly facilitated by the experimentally accessible nature of nucleic acid hybridization and characterization by gel mobility-shift, enzymatic footprinting, and enzymatic affinity cleavage methods. However, ligand-induced structural changes, linkage effects, kinetic formalisms, and energetics treatments of this study were all observed or utilized first from decades of work on protein·small molecule interactions (Levitzki, 1984; Klotz, 1986; Wyman & Gill, 1990; Weber, 1992; Kyte, 1995). Even if they have not been demonstrated similarly for combinatorial chemistry library interactions with proteins, they should be expected (Jayawickreme et al., 1994) and may impact drug discovery (Palfreyman et al., 1994). As noted earlier, both the combinatorial oligonucleotide libraries and binding sites on *ras* RNA are exceptionally structurally degenerate and this must exacerbate the linkage effects. However, enormous complexity peptide-based and small organic molecule-based libraries with high structural degeneracy have been constructed as pools (Dooley et al., 1994; Pinilla et al., 1995) and it is possible to think about combinatorial molecular recognition of protein surfaces as degenerate mapping of overlapping recognition fragments (Combs et al., 1996).

From these considerations it appears that the goal of equimolar representation of structurally degenerate members of pooled complex libraries at concentrations high enough

[2] In principle, this constraint can be satisfied as described in relationship 1, $\Sigma q[\mathrm{ULS}^*] < fK_d^* \leq [R_t]$, where $\Sigma q[\mathrm{ULS}^*]$ is the sum of the quasispecies (q) of the highest affinity unique library structures (ULS*) (oligonucleotide sequencies; *i.e.*, the three isoenergetic single nt 3′-shifted 10-mer oligonucleotides hybridizing to the 5′-most 12 nt of the *ras* loop) at the (equimolar) concentration in the screen ([ULS*]), K_d^* is the average dissociation constant for those quasispecies in bimolecular complexes with R_t, and $[R_t]$ is the concentration of target receptor (*ras* RNA). The value of f will always be less than unity and it places an upper limit on $\Sigma q[\mathrm{ULS}^*]$, and by doing so it determines the fractional saturation of R_t which may be allowed before there is undesirable linkage of binding events (perhaps $f \leq$ as high as 0.1 for the system of this study: see Figure 7 and the following section). An implicit assumption is that the values for the dissociation constants for interactions of library structures with each other will be less than or equal to the value for K_d^*, which may be reasonable for libraries containing ULS with good molecular recognition for the intended target site. Since, in practice, it generally will not be possible to know the value of either f or q, then operationally the constraints of relationship 2, $[\mathrm{ULS}^*] \ll K_d^* \leq [R_t]$, can be satisfied. When K_d^* is not known, then [ULS*] can be held fixed at a (number of) value(s) below the best expectations for K_d^* and $[R_t]$ can then be titrated over a range of values known or expected to cover the value for K_d^* in order to achieve preferential selection for ULS* in binding affinity-based screens.

for presumed single actives to provide sufficient fractional saturation of receptor molecules to be detected in bulk binding or functional assays in solution (Pinilla et al., 1995) can be problematic due to linkage effects, regardless of library composition or receptor type. In this study we have provided a conceptual solution which was experimentally verified for combinatorial oligonucleotide library screening against *ras* RNA and subsequently has been confirmed using a much longer hepatitis C virus transcript fragment (Lima et al., 1997). However, satisfaction of the constraints of this solution places severe limitations on assay formats required to detect small amounts of bimolecular complexes in the presence of largely unbound receptor. These may be unacceptable for many applications. Greater flexibility of assay utilization with higher probability of success should be achieved using any surrogate strategy that effectively restricts linkage effects by inserting seams in the structural continuum of library pools. Several approaches devised primarily to deal with practical synthetic and screening capacity limitations are already in use (Baum, 1996) and (may) have this additional benefit (but other possible limitations). These include screening library compounds singly, in very small mixtures (3 to < 30), or on solid supports, screening of multiple larger complexity pools wherein each pool has limited chemical diversity that is maximally different from that of other pools either as a result of multiple disparate syntheses or of postsynthesis fractionation, constructing pools and screening of a library in more than one way, and the use of biased, focused, or directed diversity library pools.

ACKNOWLEDGMENT

We thank Professor Olke Uhlenbeck and Dr. Heinz Moser for intellectual support and periodic critical review; Dr. Stuart Kauffman for insight and clarification of early thinking; Dr. Stanley Crooke for challenging questions; Drs. P. Dan Cook, Dave J. Ecker, and John Kiely for providing research support and resources; Elizabeth DeBaets and Dr. Pete Davis for randomized DNA library synthesis; and members of our laboratories, especially Drs. Debra Robertson and Richard Griffey, for helpful suggestions.

REFERENCES

Baum, R. (1996) *Chem. Eng. News* (Feb. 12), 28−73.

Campbell, T. B., & Cech, T. R. (1995) *RNA 1*, 598−609.

Chang, K.-Y., & Tinoco, I. (1994) *Proc. Natl. Acad. Sci. U.S.A. 91*, 8705−8709.

Chastain, M., & Tinoco, I. (1993) in *Antisense Research and Applications* (Crooke, S. T., & Lebleu, B., Eds.) pp 55−66, CRC Press, Inc., Boca Raton, FL.

Chiang, M.-Y., Chan, H., Zounes, M. A., Freier, S. M., Lima, W. F., & Bennett, C. F. (1991) *J. Biol. Chem. 266*, 18162−18171.

Cload, S. T., & Schepartz, A. (1991) *J. Am. Chem. Soc. 113*, 6324−6326.

Cload, S. T., Richardson, P. L., Huang, Y.-H., & Schepartz, A. (1993) *J. Am. Chem. Soc. 115*, 5005−5014.

Cohen, J. S., & Hogan, M. F. (1994) *Sci. Am. 271*, 76−82.

Combs, A. P., Kapoor, T. M., Feng, S., Chen, J. K., Daude-Snow, L. F., & Schreiber, S. L. (1996) *J. Am. Chem. Soc. 118*, 287−288.

Crooke, S. T., Lemonidis, K. M., Neilson, L., Griffey, R., Lesnik, E. A., & Monia, B. P. (1995) *Biochem. J. 312*, 599−608.

Davis, P., & Ecker, D. J. (1996) in *Methods in Molecular and Cellular Biology 6* (Pinilla, C., & Houghton, R. A., Eds.) pp 23−33, John Wiley and Sons, New York.

Dean, N. M., McKay, R., Condon, T. P., & Bennett, C. F. (1994) *J. Biol. Chem. 269*, 16416−16424.

Dooley, C. T., Chung, N. N., Wilkes, B. C., Schiller, P. W., Bidlack, J. M., Pasternak, G. W., & Houghton, R. A. (1994) *Science 266*, 2019−2022.

Ecker, D. J. (1993) in *Antisense Research and Applications* (Crooke, S. T., & Lebleu, B., Eds.) pp 387−400, CRC Press, Inc., Boca Raton, FL.

Ecker, D. J., Vickers, T. A., Bruice, T. W., Freier, S. M., Jenison, R. D., Manoharan, M., & Zounes, M. (1992) *Science 257*, 958−961.

Ecker, D. J., Vickers, T. A., Hanecak, R., Driver, V., & Anderson, K. (1993) *Nucleic Acids Res. 21*, 1853−1856.

Eigen, M. (1992) *Steps Towards Life. A Perspective on Evolution*, Oxford University Press, New York.

Ellington, A. D., & Szostak, J. W. (1990) *Nature 346*, 818−822.

Emerick, V. L., & Woodson, S. A. (1994) *Proc. Natl. Acad. Sci. U.S.A. 91*, 9675−9679.

Francois, J.-C., Thoung, N. T., & Helene, C. (1994) *Nucleic Acids Res. 22*, 3943−3950.

Frauendorf, A., & Engels, J. W. (1994) *Bioorg. Med. Chem. Lett. 4*, 1019−1024.

Freier, S. M. (1993) in *Antisense Research and Applications* (Crooke, S. T., & Lebleu, B., Eds.) pp 67−82, CRC Press, Inc., Boca Raton, FL.

Freier, S. M., Konings, D. A. M., Wyatt, J. R., & Ecker, D. J. (1995) *J. Med. Chem. 38*, 344−352.

Griffey, R. H., Lesnik, E., Freier, S., Sanghvi, Y. S., Teng, K., Kawasaki, A., Guinosso, C., Wheeler, P., Mohan, V., & Cook, P. D. (1994) in *Synthetic Methods and Applications in Antisense Research: An Overview. Carbohydrate Modifications in Antisense Research* (Sanghvi, Y. S., & Cook, P. D., Eds.) pp 212−224, American Chemical Society, Washington, DC.

Guinosso, C. J., Hoke, G. D., Freier, S. M., Martin, J. F., Ecker, D. J., Mirabelli, C. K., Crooke, S. T., & Cook, P. D. (1991) *Nucleosides Nucleotides 10*, 259−262.

Herschlag, D. (1991) *Proc. Natl. Acad. Sci. U.S.A. 88*, 6921−6925.

Hertel, K. J., Herschlag, D., & Uhlenbeck, O. C. (1994) *Biochemistry 33*, 3374−3385.

Jaeger, J. A., SantaLucia, J., & Tinoco, I. (1993) in *Annual Review of Biochemistry* (Richardson, C. C., Abelson, J. N., Meister, A., & Walsh, C. T., Eds.) pp 255−287, Annual Reviews, Inc., Palo Alto, CA.

Jaroszewski, J. W., Syi, J.-L., Ghosh, M., Ghosh, K., & Cohen, J. S. (1993) *Antisense Res. Dev. 3*, 339−348.

Jayawickreme, C. K., Graminski, G. F., Quillan, J. M., & Lerner, M. R. (1994) *Proc. Natl. Acad. Sci. U.S.A. 91*, 1614−1618.

Jones, J. T., Lee, S.-W., & Sullenger, B. A. (1996) *Nature Med. 2*, 643−648.

Klotz, I. M. (1986) *Introduction to Biomolecular Energetics, Including Ligand−Receptor Interactions*, Academic Press, New York.

Kyte, J. (1995) *Mechanism in Protein Chemistry*, Garland Publishing, New York.

Ladbury, J., & Peters, R. (1994) *Bio/Technol. 12*, 1083−1085.

LaGrandeur, T. E., Huttenhofer, A., Noller, H. F., & Pace, N. R. (1994) *EMBO J. 3*, 3945−3952.

Lesnik, E. A., Guinosso, C. J., Kawasaki, A. M., Sasmor, H., Zounes, M., Cummins, L. L., Ecker, D. J., Cook, P. D., & Freier, S. M. (1993) *Biochemistry 32*, 7832−7838.

Levitzki, A. (1984) *Receptors. A Quantitative Approach*, Benjamin/Cummings, Menlo Park, CA.

Lieber, A., & Strauss, M. (1995) *Mol. Cell Biol. 15*, 540−551.

Lima, W. F., Monia, B. P., Ecker, D. J., & Freier, S. M. (1992) *Biochemistry 31*, 12055−12061.

Lima, W. F., Brown-Driver, V., Fox, M., Hanecak, R., & Bruice, T. W. (1997) *J. Biol. Chem. 272*, 626−638.

Lingner, J., Hendrick, L. L., & Cech, T. R. (1994) *Genes Dev. 8*, 1984−998.

Loke, S. L., Stein, C. A., Zhang, X. H., Mori, K., Nakanishi, M., Subasinghe, C., Cohen, J. S., & Neckers, L. M. (1989) *Proc. Natl. Acad. Sci. U.S.A. 86*, 3474−3478.

Monia, B. P., Johnston, J. F., Ecker, D. J., Zounes, M. A., Lima, W. F., & Freier, S. M. (1992) *J. Biol. Chem. 267*, 19954−19962.
Nellen, W., & Lichtenstein, C. (1993) *Trends. Biochem. Sci. 18*, 419−423.
Palfreyman, M. G., Reynolds, I. J., & Skolnick, P., Eds. (1994) *Direct and Allosteric Control of Glutamate Receptors*, CRC Press, Boca Raton, FL.
Pinilla, C., Appel, J., Blondelle, S., Dooley, C., Dorner, B., Eichler, J., Ostresh, J., & Houghton, R. A. (1995) *Biopolymers (Pept. Sci.) 37*, 221−240.
Porta, H., & Lizardi, P. M. (1995) *Bio/Technology 13*, 161164.
Richardson, P. L., & Schepartz, A. (1991) *J. Am. Chem. Soc. 113*, 5109−5111.
Rittner, K., Burmester, C., & Sczakiel, G. (1993) *Nucleic Acids Res. 21*, 1381−1387.
Robertson, D. L., & Joyce, G. F. (1990) *Nature 344*, 467−468.
Rose, I. A. (1980) in *Methods in Enzymology, Enzyme Kinetics and Mechanism, Part B* (Purich, D. L., Ed.) p 47, Academic Press, New York.
Sczakiel, G., Homann, M., & Rittner, K. (1993) *Antisense Res. Dev. 3*, 45−52.
Southern, E. M., Case-Green, S. C., Elder, J. K., Johnson, M., Mir, K. U., Wang, L., & Williams, J. C. (1994) *Nucleic Acids Res. 22*, 1368−1373.
Stein, C. A., & Krieg, A. M. (1994) *Antisense Res. Dev. 4*, 67−69.
Stenesh, J. (1993) *Core Topics in Biochemistry*, Cogno Press, Kalamazoo, MI.
Tuerk, C., & Gold, L. (1990) *Science 249*, 505−510.
Wagner, R. W. (1994) *Nature 372*, 333−335.
Wagner, R. W., Matteucci, M. D., Grant, D., Huang, T., & Froehler, B. C. (1996) *Nat. Biotechnol. 14*, 840−844.
Weber, G. (1992) *Protein Interactions*, Chapman and Hall, New York.
Weeks, K. M., & Crothers, D. M. (1992) *Biochemistry 31*, 10281−10287.
Weidner, D. A., & Busch, H. (1994) *Oncology Res. 6*, 237−242.
Woolf, T. M., Melton, D. A., & Jennings, C. G. B. (1992) *Proc. Natl. Acad. Sci. U.S.A. 89*, 7305−7309.
Wu-Pong, S. (1994) *Pharm. Technol 18*, 102−114.
Wyman, J., & Gill, S. J. (1990) *Binding and Linkage. Functional Chemistry of Biological Macromolecules*, University Science Books, Mill Valley, CA.

BI9620767